JGR Biogeosciences

RESEARCH ARTICLE
10.1029/2022JG007107

Shrubs Compensate for Tree Leaf Area Variation and Influence Vegetation Indices in Post-Fire Siberian Larch Forests

Nadav S. Bendavid[1,2], Heather D. Alexander[3], Sergei P. Davydov[4], Heather Kropp[5], Michelle C. Mack[6], Susan M. Natali[7], Seth A. Spawn-Lee[8], Nikita S. Zimov[4], and Michael M. Loranty[1]

[1]Department of Geography, Colgate University, Hamilton, NY, USA, [2]Now at: School of the Environment, Yale University, New Haven, CT, USA, [3]College of Forestry, Wildlife, and Environment, Auburn University, Auburn, AL, USA, [4]Pacific Geographical Institute, Far East Branch, Russian Academy of Sciences, Northeast Science Station, Cherskiy, Russia, [5]Environmental Studies Program, Hamilton College, Clinton, NY, USA, [6]Center for Ecosystem Science and Society, Northern Arizona University, Flagstaff, AZ, USA, [7]Woodwell Climate Research Center, Falmouth, MA, USA, [8]Department of Geography, University of Wisconsin, Madison, WI, USA

Key Points:

- Tall shrubs compensate for lower tree leaf area in low density larch forests
- Combined leaf area of trees and tall shrubs is consistent across a range of forest tree densities
- Satellite-derived vegetation indices are more closely linked to shrub LAI than tree LAI or combined tree-shr LAI

Correspondence to:

N. S. Bendavid,
nadav.bendavid@yale.edu

Citation:

Bendavid, N. S., Alexander, H. D., Davydov, S. P., Kropp, H., Mack, M. C., Natali, S. M., et al. (2023). Shrubs compensate for tree leaf area variation and influence vegetation indices in post-fire Siberian larch forests. *Journal of Geophysical Research: Biogeosciences*, *128*, e2022JG007107. https://doi.org/10.1029/2022JG007107

Received 23 JUL 2022
Accepted 13 FEB 2023

Abstract In post-fire Siberian larch forests, where tree density can vary within a burn perimeter, shrubs constitute a substantial portion of the vegetation canopy. Leaf area index (LAI), defined as the one-sided total green leaf area per unit ground surface area, is useful for characterizing variation in plant canopies. We estimated LAI with allometry for trees and tall shrubs (>0.5 and <1.5 m) across 26 sites with varying tree stem density (0.05–3.3 stems/m^2) and canopy cover (4.6%–76.9%) in a uniformly-aged mature Siberian larch forest that regenerated following a fire ~75 years ago. We investigated relationships between tree density, tree LAI, and tall shrub LAI, and between LAI and satellite observations of Normalized Difference and Enhanced Vegetation Indices (NDVI and EVI). Across the density gradient, tree LAI increases with increasing tree density, while tall shrub LAI decreases, exhibiting no patterns in combined tree-shrub LAI. We also found significant positive relationships between tall shrub LAI and NDVI/EVI from PlanetScope and Landsat imagery. These findings suggest that tall shrubs compensate for lower tree LAI in tree canopy gaps, forming a canopy with contiguous combined tree-shrub LAI across the density gradient. Our findings suggest that NDVI and EVI are more sensitive to variation in tall shrub canopies than variation in tree canopies or combined tree-shrub canopies in these ecosystems. The results improve our understanding of the relationships between forest density and tree and shrub leaf area and have implications for interpreting spatial variability in LAI, NDVI, and EVI in Siberian boreal forests.

Plain Language Summary After wildfires burn forests in northeast Siberia, they often grow back unevenly, with some sections containing many more trees than others. Sections with more trees have a higher capacity to take up carbon and higher rates of energy production, which has important implications for climate change. To investigate how vegetation varies across sections of a forest which burned in 1940, we estimated the separate and combined contributions of trees and tall shrubs (>0.5 and <1.5 m) in high, medium, and low density sections using tree and shrub stem diameter measurements. We estimated the canopy vegetation in each section of forest by calculating the total area of leaves in the section and dividing it by the total ground area, producing the leaf area index (LAI). In sections with less dense tree cover, tall shrubs made up for lower tree leaf area, and the combined leaf area of trees and tall shrubs was consistent across the sections of different tree density. We also compared our leaf area measurements with measures of vegetation productivity produced from satellite imagery, finding that the satellite measures were correlated with tall shrub LAI, but not with tree LAI or combined LAI from trees and shrubs.

1. Introduction

A large and growing body of research suggests that the magnitude of warming due to anthropogenic climate change in the Arctic is four times the global average (Previdi et al., 2021; Rantanen et al., 2022; Serreze & Barry, 2011). This Arctic amplification is partly due to sea ice loss across the Arctic, which decreases regional albedo and amplifies warming, a process known as the sea ice–albedo feedback (Hudson, 2011; Perovich & Polashenski, 2012; Previdi et al., 2021; Winton, 2006). The extreme magnitude of this warming drives ongoing shifts in Arctic vegetation, with shrubs and trees increasing cover in areas previously consisting of graminoid

tundra (Elmendorf et al., 2012; Macias-Fauria et al., 2012; Tape et al., 2006). Satellite observations show greening trends consistent with these shifts (Berner et al., 2020; Berner & Goetz, 2022; Myers-Smith et al., 2020), and vegetation modeling predicts increased woody cover across the Arctic by over 50%, with changes in physiognomic class to at least half of all vegetated areas by 2050 (Pearson et al., 2013). These changes could further decrease albedo as growing season length and the snow-masking effects of vegetation increase in magnitude, causing further amplification of warming in the Arctic (Pearson et al., 2013). In addition to direct stimulation of vegetation growth, rising temperatures have wide-reaching ecological ramifications in the Arctic as they drastically alter many fundamental geophysical processes such as wildfire and permafrost freeze-thaw cycles, with consequent changes in vegetation cover and composition.

Changing climate indirectly impacts boreal forests through increased wildfire extent, frequency and severity (Groisman et al., 2007; Johnstone et al., 2016; Johnstone & Kasischke, 2005; Z. Liu et al., 2012; Ponomarev et al., 2016; Stocks et al., 1998). Unusual wildfire events can function as a trigger of vegetation change in fire-dependent ecosystems, as more severe fires driven by warming climate alter the seedbed through the exposure of more mineral soils, promoting the germination and establishment of light-seeded hardwood trees over more heavily seeded conifers (Cai et al., 2013; Groisman et al., 2007; Johnstone et al., 2016; Johnstone & Kasischke, 2005; Ponomarev et al., 2016; Stocks et al., 1998). This phenomenon is well-studied in North American boreal forests, where wildfire has facilitated shifts from conifer-dominance to the dominance of deciduous broadleaf species, altering the spatial distribution of carbon (Johnstone, Chapin, et al., 2010; Johnstone, Hollingsworth, et al., 2010; Mack et al., 2021). However, the role of wildfire in the facilitation of vegetation shifts remains largely unexplored in Siberia, where the majority of continuous permafrost occurs within the boreal forest biome. In monodominant Cajander larch (*Larix cajanderi* Mayr.) boreal forests of northeast Siberia, stand-replacing fires play an essential role in ecological succession (Alexander et al., 2012; Shorohova et al., 2009; Valendik & Ivanova, 2001). Instead of alternate successional trajectories driven by changes in tree functional types like those commonly seen in North America, forest trajectories can vary depending on forest tree density in relation to shrub cover (Alexander et al., 2012, 2018), given the differences in species assemblages between North American and Siberian forests. In northeast Siberia, tall deciduous shrubs (>0.5 and <1.5 m), particularly *Betula nana* L. and *Salix* spp., are abundant where tree density is low (Paulson et al., 2021). Fire is widespread in the region, with fire frequency (Ponomarev et al., 2016) and burned area (Talucci et al., 2022) increasing in response to climatic changes, yet the extent to which large scale shifts in tree density occur remains unclear.

Plant canopies, which serve as a primary interface between the atmosphere and the biosphere, are key to understanding how variation in ecosystem structure might relate to climate feedbacks with albedo (Bonan et al., 1992; Webb et al., 2021), water and energy exchange (Beringer et al., 2005), and CO_2 uptake capacity (Ollinger et al., 2008; Richardson et al., 2013). Leaf area index (LAI) is a key parameter in the modeling of earth system processes in the Arctic, particularly the cycling and dynamics of carbon (e.g., Birch et al., 2021; Ueyama, Ichii, et al., 2013; Ueyama, Iwata, et al., 2013), and water (e.g., Hedstrom & Pomeroy, 1998; Launiainen et al., 2019; Parajuli et al., 2020). LAI is defined as the one-sided total green leaf area per unit ground surface area (J. M. Chen & Black, 1992; Fernandes et al., 2014), agreeing with the definition of LAI for flat-needled trees (i.e., *L. cajanderi*) used in calculating the Moderate Resolution Imaging Spectroradiometer (MODIS) LAI product (Myneni et al., 1997, 2015). Typically, LAI is estimated indirectly for the entire canopy through the use of optical methods, but it can also be estimated directly through the use of allometric relationships (J. M. Chen et al., 1997; Gower et al., 1999; Jonckheere et al., 2004).

In the context of modeling ecosystem processes, remote sensing is often used to infer spatial and temporal variability in canopy LAI. This approach can be challenging in many contexts, as the relationship between ground-based LAI values and satellite-derived vegetation indices (VIs) such as the Normalized Difference and Enhanced Vegetation Indices (NDVI and EVI, respectively) is highly variable depending on factors that include the time of year, the statistical methods used to derive the indices, background NDVI levels, and the temporal scale of measurement (J. M. Chen & Cihlar, 1996; Cohen et al., 2003; Wang et al., 2005). Research conducted at the same Siberian larch forest used in this study demonstrates that remotely sensed VIs do not capture variation in forest cover, finding that NDVI and EVI are both unrelated to field observations of tree canopy cover and biomass (Loranty, Davydov, et al., 2018). Some remote sensing products estimate LAI directly without the use of NDVI or EVI as a proxy, such as the MODIS LAI product (MOD15) and the Polarization and Directionality of the Earth's Reflectance (POLDER) LAI maps. However, when assessed for accuracy in boreal forests, MODIS

overestimated LAI for forests early in post-fire succession and underestimated it for later successional forests (X. Chen et al., 2005; Serbin et al., 2013; Verbyla, 2005), while POLDER generally underestimated LAI (Abuelgasim et al., 2006). Given the uncertainty of satellite-derived VIs to accurately reflect post-fire LAI variation, analyses of variation in LAI and vegetation dynamics using ground-based allometry data are very valuable. They are particularly useful for understanding vegetation-climate feedbacks in the context of vegetation shifts, especially in high-latitude ecosystems experiencing amplified warming.

In this study, we investigate variation in plant canopies across a monodominant upland Siberian larch forest, examining the separate and combined contributions of trees and tall shrubs (>0.5 and <1.5 m) to LAI. While prostrate shrubs and other non-woody vegetation types are found in the understory, tall shrubs are most abundant and vary with forest density (Paulson et al., 2021). We use tree and tall shrub stem measurements from 26 similarly-aged, mature stands along a gradient varying in larch stem density and located within the perimeter of a single wildfire that occurred ca. 1940 (Paulson et al., 2021). We estimate LAI for trees and tall shrubs using site- and genus/species-specific allometric equations and examine the relationships between tree and tall shrub LAI, and two commonly used satellite-derived proxies for vegetation productivity, the NDVI and EVI, respectively. By analyzing variation in LAI across the tree density gradient, and comparing that data to satellite vegetation indices, we aim to address the following questions: (a) How do tree LAI, tall shrub LAI, and combined tree-shrub LAI vary across a post-fire tree density gradient? and (b) How do the commonly used vegetation indices NDVI and EVI relate to variation in tree LAI, tall shrub LAI, and combined tree-shrub LAI? We expect tree LAI to increase with increasing tree stem density while tall shrub LAI decreases. Overall, we expect combined tree-shrub LAI to increase with tree stem density, with tall shrubs partially compensating for lower tree LAI at less dense stands. We do not expect to find a relationship between variation in LAI and variation in NDVI or EVI, given the lack of relationships between satellite-derived VIs, larch canopy cover, and larch biomass observed in previous research at this study site (Loranty, Davydov, et al., 2018).

2. Methods

2.1. Study Site

The study was conducted in Siberia near the Northeast Science Station (NESS) in Cherskiy, Sakha Republic, Russian Federation (68.76°N, 161.46°E; Figure 1). The climate is cold with mean annual, summer, and winter temperatures of −10.5°C, 10.9°C, and −31.3°C, respectively for the 1991–2020 reference period (Paulson et al., 2021). Data gaps in precipitation observations submitted to the Global Historical Climatology Network preclude calculation precipitation sums for the same reference period, however Berner et al. (2013) report mean total annual precipitation of 282 mm using CRU data for the 1938–2009 reference period. The region is underlain by continuous permafrost. Forests are composed exclusively of Cajander larch trees, a deciduous conifer that is fire adapted with non-serotinous cones and wind-dispersed seeds. Understory vegetation includes tall erect shrubs (*Betula* spp. and *Salix* spp.), short evergreen shrubs (*Vacciunium vitis idaea*, *Empetrum nigrum*, and *Rhododendron tomentosum (*syn. *Ledum palustre)*), mosses (*Aulacomnium* spp. and *Polytrichum* spp.), and lichens (*Cladonia rangiferina*, *Cetraria cuculata*, and *Stereocaulon tomentosum*) (Paulson et al., 2021). Wildfire is required for larch germination, reducing competition and improving seedbed conditions by exposing the soil mineral layer (Alexander et al., 2018). More than half (50%–60%) of fires in the region are stand-replacing, destroying existing larch vegetation through the root layer and leading to the development of a consistently aged cohort (Alexander et al., 2018; Sofronov & Volokitina, 2010). Historically, stand-replacing fires have occurred every 80–300 years (Krylov et al., 2014), but climate change is driving increases in fire frequency, extent, and prevalence (Ponomarev et al., 2016).

To examine how variation in tree density affects LAI in an evenly-aged monodominant larch forest, we sampled trees and tall shrubs within the perimeter of a fire that burned ca. 1940. Forests within the burn perimeter exhibit a wide range of tree stem densities, with stands grouped as low (<3,500 stems/ha), medium (≥3,500 and <10,000 stems/ha), and high (≥10,000 stems/ha) density (Paulson et al., 2021; X. J. Walker et al., 2021). High density stands have an average of 2.12 stems/m^2, 64.1% canopy cover, and 1,828.8 g aboveground biomass; medium density stands have an average of 0.71 stems/m^2, 40.5% canopy cover, and 1,271.5 g aboveground biomass; low density stands have an average of 0.16 stems/m^2, 17.9% canopy cover, and 431.3 g aboveground biomass (Table 1). The variation in larch stem density is likely a consequence of the combined effects of variation in burn severity and seed availability (Alexander et al., 2018; Paulson et al., 2021). Most trees within these stands

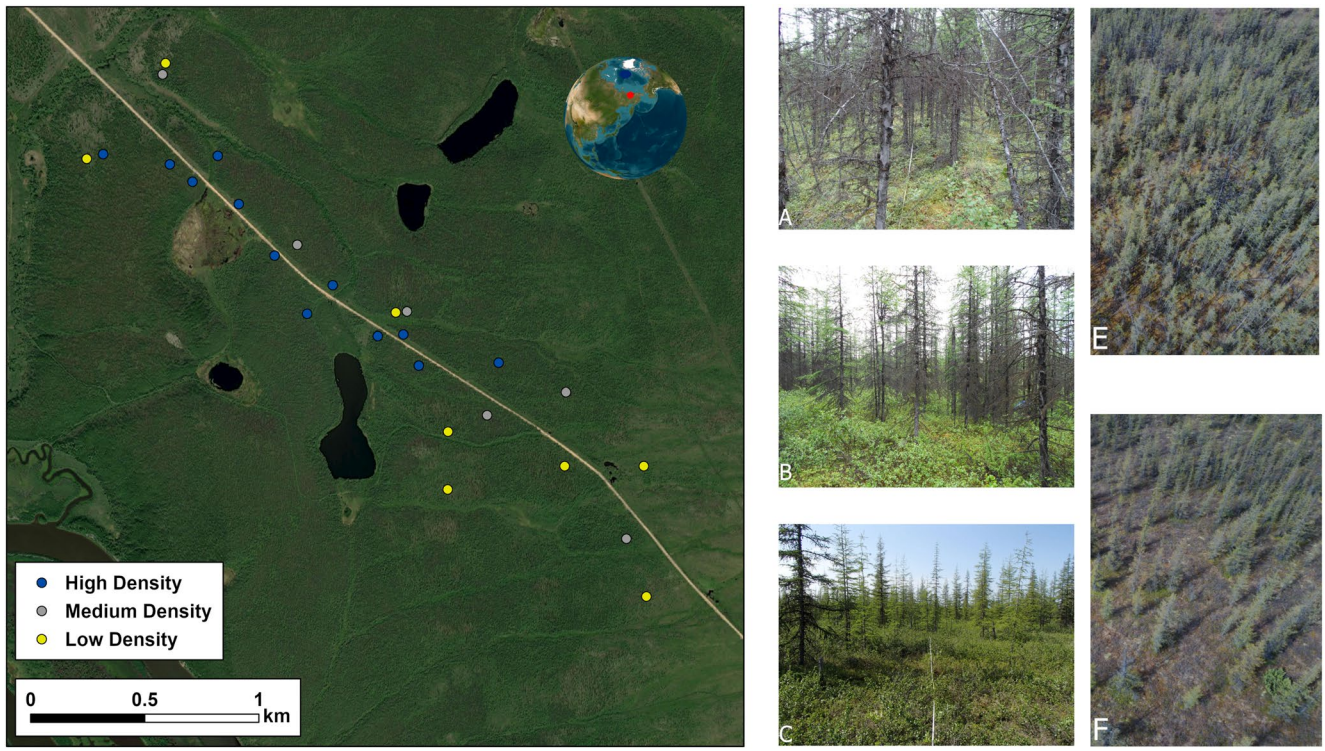

Figure 1. The left panel shows a map of the study sites denoting the different density classes. Illustrative photos on the right panel show representative high-density (a), medium-density (b), and low-density sites (c), along with aerial photos of high-density (e) and low-density (f) sites.

originated between 10 and 15 years post-fire, and surveys of standing dead and coarse woody debris indicate a uniform low-density stand existed across the area before the fire (Paulson et al., 2021).

2.2. Field Data

We used high-resolution satellite imagery and field reconnaissance to identify 26 stands within the burn perimeter that spanned a range of post-fire tree density (Figure 1). During the summers of 2014–2017, we conducted detailed vegetation inventories at each stand. Our sampling was conducted along three 30 m long belt transects spaced ~30 m apart, with widths ranging from 1 to 8 m depending on tree density, creating plots ranging in area from 30 to 240 m^2. Within each belt transect we recorded the diameter at breast height (DBH) for every live tree. We sampled tall shrubs (>0.5 and <1.5 m) using a subplot with a length of 5 m nested within each belt transect. Subplots began at one end of each transect and had widths ranging from 0.5 to 4 m depending on stem density, creating subplots ranging in area from 2.5 to 20 m^2. Tall shrub stem density was generally quite high, so subplots with lengths >5 m would have been redundant. Within each tall shrub subplot, the basal diameter (BD) of all live tall shrubs was recorded.

Table 1
Mean Stand Characteristics by Density Class

Stand density class	Mean characteristic ± Standard error		
	Tree stem density (stems/m^2)	Canopy cover (%)	Aboveground biomass (g)
High	2.121 ± 0.321	64.106 ± 3.842	1,828.797 ± 248.089
Medium	0.706 ± 0.136	40.540 ± 4.897	1,271.487 ± 260.053
Low	0.164 ± 0.055	17.907 ± 3.486	431.275 ± 247.156

2.3. Allometry

We estimated LAI from tree and tall shrub stem diameter measurements using locally-calculated, genus/species-specific allometric relationships (Alexander et al., 2012; Berner et al., 2015). Using the general equation for leaf mass, $LM = ax^b$, where x represents BD or DBH, and a and b represent genus/species-specific parameters (see Table 2), we estimated leaf mass for each tree and tall shrub. Next, we multiplied leaf mass by mean specific leaf area (SLA) to estimate total leaf area for each individual (Kropp et al., 2019). Finally, we summed the total leaf area for all individuals in each belt transect and divided the sum by transect ground area to estimate LAI for each transect.

Table 2
Allometric Parameters and Specific Leaf Area by Species

Species	Allometric parameters			Specific leaf area (cm^3/g)	
	Diameter type	*a*	*b*	High density	Low density
Larix cajanderi	BD	22.55[a]	1.45[a]	112.89[b]	84.69[b]
	DBH	40.50[a]	1.41[a]		
Betula nana	BD	4.57[c]	2.45[c]	167.44[d]	126.55[d]
Salix spp.	BD	3.11[c]	2.18[c]	145.48[d]	127.02[d]

[a]Alexander et al., 2012. [b]Kropp et al., 2019. [c]Berner et al., 2015. [d]Data collected by authors.

We used the mean of the three transects in each stand as the stand-level LAI value.

We calculated separate allometric equations for high- and low-density stands because canopy architecture and allocation patterns likely varied due to different levels of competition for resources. Medium-density stands are essentially clumps of high-density forest, so SLA values for high-density were used for these stands. SLA values for trees and tall shrubs were derived from leaves and needles sampled at high- and low-density study sites during the 2016 and 2017 field seasons (Kropp & Loranty, 2018). We performed leaf mass allometry using existing equations derived from destructive harvest of trees and shrubs at the study sites, as well as from similar nearby sites. To estimate tall shrub leaf mass we used genus/species-specific equations from Berner et al. (2015) that were calculated using shrubs from sites in the region, including our study sites. For tree leaf mass at low-density sites we used equations reported by Alexander et al. (2012) that were derived from destructive harvests at a similar nearby site (Kajimoto et al., 2006). Equations for high-density leaf mass were developed by Kropp et al. (2019) from destructive harvests at our study sites.

2.4. Satellite Data

To investigate relationships between LAI and satellite-derived VIs, we used imagery from the PlanetScope and Landsat satellite platforms. We used a single Landsat 8 OLI image acquired on 28 July 2017, and a single PlanetScope image acquired on 26 July 2017. Both images were also used for comparison of forest cover and VIs by Loranty, Davydov, et al. (2018). The Landsat scene from WRS Path 105 Row 12 was processed to Surface Reflectance and acquired from the USGS EarthExplorer, and has a spatial resolution of 30 m. We used the included cloud mask to exclude clouds and shadows and applied an NDVI threshold of 0.5 to exclude cloud shadows missed by the mask. Masking did not remove data from any of our study sites. PlanetScope captures imagery in blue, green, red, and NIR spectral bands at 3 m spatial resolution (Planet Team, 2017). The Planet Surface Reflectance product is derived by atmospherically correcting the top-of-atmosphere reflectance product using a radiative transfer model informed by concurrent MODIS scenes (Vermote et al., 1997). The Planet image was manually screened for cirrus or haze contamination. NDVI was calculated using NIR and Red reflectances as follows:

$$\mathrm{NDVI} = \frac{\mathrm{NIR} - \mathrm{Red}}{\mathrm{NIR} + \mathrm{Red}}$$

EVI was calculated using NIR, Red, and Blue reflectances as follows:

$$\mathrm{EVI} = 2.5 \times \frac{\mathrm{NIR} - \mathrm{Red}}{(\mathrm{NIR} + 6) \times (\mathrm{Red} - 7.5) \times (\mathrm{Blue} + 1)}$$

For analysis we extracted data from all pixels within a 15 m radius of plot centers from Landsat and Planet NDVI and EVI images. For Landsat imagery, the radius was approximately one pixel and for Planet imagery the radius was approximately five pixels, using a weighted average to aggregate any data beyond the 15 m radius. The radius of 15 m was selected as it encompasses all the transects without exceeding the sampled area or including areas where edge effects could have skewed results due to proximity to a road.

2.5. Data Analysis

We processed field data and satellite images and performed all data analyses with R 4.0.3 (R Core Team, 2020). To find the significance of differences in mean allometric LAI across sites of high, medium, and low density, we performed one-way analysis of variance (ANOVAs) of tree, shrub, and combined tree-shrub LAI using the aov function in R. A post-hoc Tukey's honest significance test was performed on each ANOVA to calculate the significance of the difference between each combination of densities. We also performed a linear regression of the relationship between tree and shrub LAI using the lm function in R. We used the same function to perform

Table 3
Allometric LAI for Tree and Tall Shrub Species at High, Medium, and Low Density Stands

	Mean LAI ± standard error (m^2/m^2)				
		Tall shrubs			
Stand density class	Trees (*L. cajanderi*)	*Salix* spp.	*Betula* spp.	Total tall shrubs	Trees + shrubs
High	1.294 ± 0.364^{a}	0.018 ± 0.025	0.124 ± 0.121^{a}	0.134 ± 0.123^{a}	1.43 ± 0.487
Medium	0.819 ± 0.397^{bc}	0.030 ± 0.037	0.341 ± 0.156^{bc}	0.362 ± 0.172^{bc}	1.18 ± 0.569
Low	0.663 ± 0.599^{c}	0.042 ± 0.049	0.447 ± 0.217^{c}	0.487 ± 0.225^{c}	1.15 ± 0.824

Note. Superscript letters indicate significance ($p < 0.05$) from Tukey's honest significance test.

linear regressions of the relationships between EVI and NDVI, and tree, shrub, and combined tree-shrub LAI. The raster (Hijmans, 2020) and rgdal (Bivand et al., 2020) packages were used for processing satellite imagery, and the ggplot2 (Wickham, 2016) package was used to generate data visualizations.

3. Results

3.1. Allometry and Canopy Composition

Allometry revealed an inverse relationship between tree LAI and tall shrub LAI, with tree LAI increasing with stands of increasing tree density. The SLA values used in allometric calculations are presented in Table 2 for each genus/species at high and low tree density stands. Mean LAI values from allometry by tree density, vegetation type (tree vs. tall shrub), and species are reported in Table 3. In high density stands, 90% of combined tree-shrub LAI (1.4 m^2/m^2) was due to trees (1.3 m^2/m^2), with only 10% due to tall shrubs (0.13 m^2/m^2). In medium density stands, 69% of total LAI (1.2 m^2/m^2) was due to trees (0.82 m^2/m^2), and 31% was due to tall shrubs (0.36 m^2/m^2). In low density stands, 58% of total LAI (1.2 m^2/m^2) was due to trees (0.66 m^2/m^2), and 42% was due to tall shrubs (0.49 m^2/m^2). *Betula* spp. contributed 87%, 92%, and 91% of tall shrub LAI at high, medium, and low densities, respectively, with *Salix* spp. contributing the remainder of tall shrub LAI. We found significant differences in mean tree LAI (Figure 2a; $F_{2,77} = 16.02$; $p < 0.001$) and tall shrub LAI (Figure 2b; $F_{2,69} = 29.52$; $p < 0.001$) between high, medium, and low density sites. The differences in mean combined tree-shrub LAI between different densities were not significant (Figure 2c, $F_{2,80} = 1.34$; $p = 0.27$). We also found a significant negative relationship between tall shrub LAI and tree LAI, represented by the model $s = -0.24t + 0.54$, where s is tall shrub LAI and t is tree LAI (Figure 3; $R^2 = 0.28$, $p = 0.007$).

3.2. Leaf Area Index and Satellite VIs

We found significant positive linear relationships between tall shrub LAI and Planet NDVI (Figure 4c, $p = 0.002$, $r = 0.47$), as well as tall shrub LAI and Landsat NDVI (Figure 5c, $p = 0.02$, $r = 0.59$). We also observed significant positive relationships between tall shrub LAI and Planet EVI (Figure 4d, $p = 0.005$, $r = 0.57$), and tall shrub LAI and Landsat EVI (Figure 5d, $p = 0.003$, $r = 0.56$). Additionally, there was a significant negative relationship between tree LAI and Landsat EVI (Figure 5b, $p = 0.008$, $r = -0.53$). Relationships between tree LAI and Landsat NDVI, tree LAI and Planet NDVI/EVI, and combined tree-shrub LAI and Landsat and Planet NDVI/EVI were not significant.

4. Discussion

4.1. What Are the Implications of Tree-Shrub LAI Compensation?

Mean tree LAI and tall shrub LAI differed significantly between sites of high, medium, and low larch density, but combined tree-shrub LAI did not. Additionally, we found a significant negative correlation between mean tree LAI and tall shrub LAI. These findings suggest that the role of tall shrubs in this larch forest canopy is compensatory, providing a higher proportion of combined tree-shrub LAI in stands with lower tree LAI due to lower tree density. Furthermore, this tall shrub compensation creates a canopy of consistent combined tree-shrub LAI across the gradient of tree density. The phenomenon of tree-shrub LAI compensation has not been documented

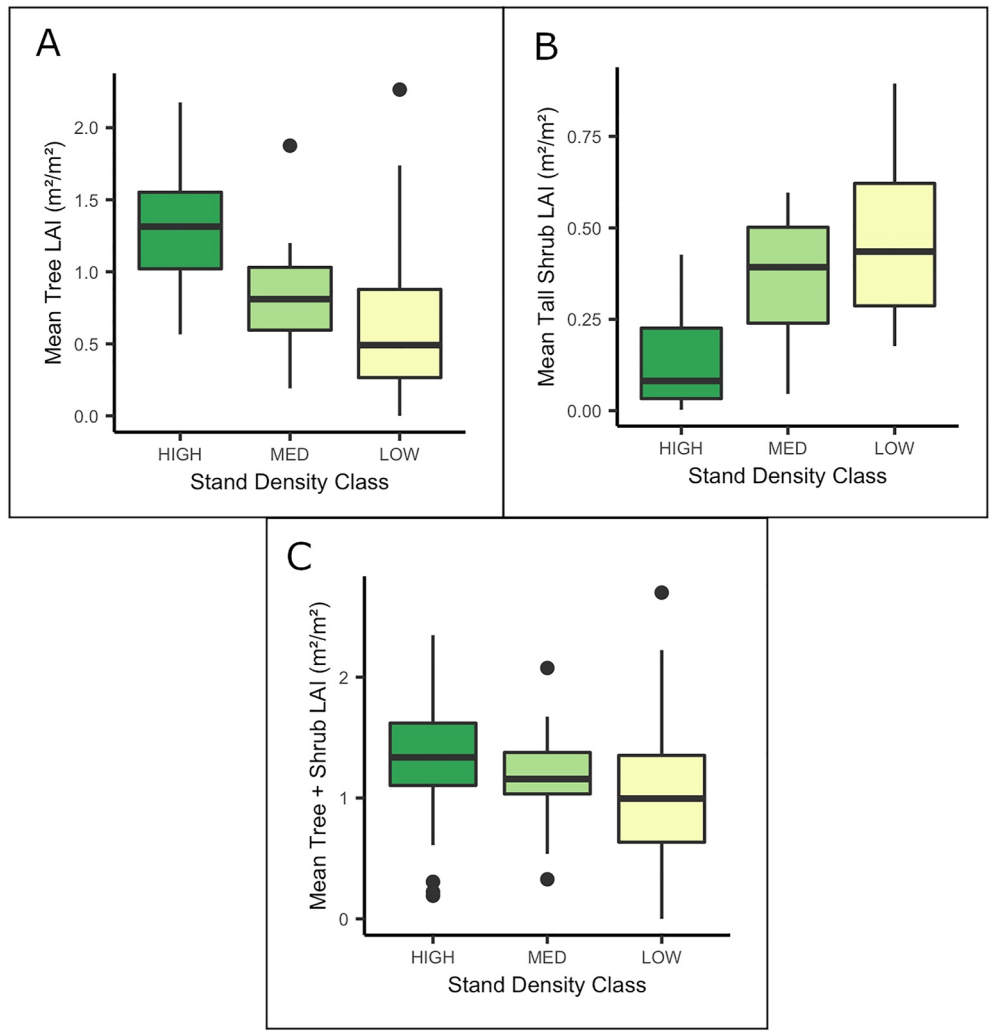

Figure 2. Mean leaf area index (LAI) for trees (a), tall shrubs (b), and trees + shrubs (c) for forest stands in high, medium, and low density classes.

before and has potential implications for interpreting measures of LAI, as well as remotely sensed VIs, when the contributions of tall shrubs and trees to total canopy LAI have not been evaluated separately. When interpreting LAI products derived from satellite imagery, our results provide insight as to how tree and tall shrub LAI relate to each other and to tree stem density for a Cajander larch forest.

Variation in tree and tall shrub LAI across the tree density gradient likely drives variation in understory composition, diversity, and abundance. Paulson et al. (2021) surveyed understory characteristics across the same tree density gradient, finding insignificant variation in graminoid, herb, lichen, and short shrub abundance, a positive relationship between tree density and moss abundance, and a negative relationship between tree density and tall shrub abundance. They also report that when active layer depth and soil organic layer (SOL) depth are at their mean values, species richness decreases with increasing larch density, a pattern typically attributed to lower resource availability at high density stands (Bartels & Chen, 2010; Euskirchen et al., 2006; Grandpré et al., 1993). This suggests that the relationship between LAI and understory biodiversity is dependent on whether the canopy is dominated by trees or tall shrubs, with tall shrub canopies supporting higher understory biodiversity. Even if combined tree-shrub LAI is equal across the tree density gradient, the structural differences between columnar tree and clumped tall shrub canopies likely drive variation in understory light availability. Mosses are significant components of understory communities and can have high leaf areas (Bond-Lamberty & Gower, 2007; Turetsky et al., 2012), but there is an absence of high-quality data for moss abundance and leaf area in Siberian boreal forests.

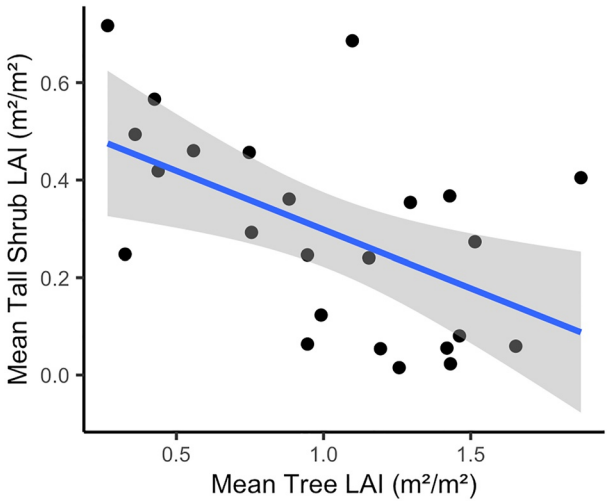

Figure 3. Linear regression of the significant relationship between mean tree and tall shrub leaf area index (LAI) by plot. For this regression, $R^2 = 0.28$, $p < 0.05$.

Graminoids, herbs, lichens, mosses, and short shrubs all likely contribute to total ecosystem LAI in addition to trees and tall shrubs. However, as noted above, point-intercept surveys of understory vegetation at our study sites illustrate that only tall shrubs and moss vary proportionally with tree density, while graminoids, herbs, lichens, and short shrubs are equally abundant across the density gradient (Paulson et al., 2021). This, combined with the relatively low abundance of these functional types relative to trees and shrubs, makes it reasonable to assume that their contributions to LAI and impacts on VIs are also relatively small and similar across sites. Moss abundance increased with tree density (Paulson et al., 2021), and may therefore have varying contributions to total ecosystem LAI. However, in high density forests where mosses are most abundant, they would likely be obscured by the tree canopy making their effects on VIs unclear.

4.2. Leaf Area Index and Satellite-Derived VIs

We found significant, positive relationships between tall shrub LAI and NDVI, as well as between tall shrub LAI and EVI, using both PlanetScope and Landsat imagery. Relationships between tree LAI and VIs were insignificant. NDVI and EVI were both included in these analyses because NDVI is commonly used to examine boreal vegetation dynamics, while EVI offers improvements in accounting for the effects of soil and other potentially confounding factors, presenting rationale to compare the indices in this context. We observed discrepancies between the absolute values of VIs derived from Landsat and Planet imagery that may be due to differences in product resolution and band wavelength, as documented in other types of forest (Härkönen et al., 2015; Y. Liu et al., 2018; Ogutu et al., 2012), or due to atmospheric corrections and/or differences in illumination and viewing geometry. Our focus was on spatial variability between sites, and the patterns we observed are consistent between the imagery sources, so we did not further investigate or attempt to account for or correct differences between sensors. The consistency of our results suggests that tall shrub canopies influence satellite-derived VIs more strongly than larch canopies, a finding that is in line with previous research at our sites demonstrating no link between either NDVI or EVI and larch biomass or canopy cover (Loranty, Davydov, et al., 2018). A possible explanation for this relationship is that tall shrub canopies are distributed less vertically and more horizontally than tree canopies. Thus, a larger proportion of the leaf area of tall shrub canopies is visible to satellite sensors than the leaf area of tree canopies. Additionally, the more vertically distributed tree canopies include a larger proportion of non-photosynthetic tissue (i.e., stems and branches) than shrub canopies. The negative relationship we found between tree LAI and EVI may also reflect the higher proportion of non-photosynthetic material in trees than in shrubs.

We estimated LAI using site- and species-specific allometric equations, rather than more commonly employed optical methods. Optical methods use light transmission to measure the gap fraction of the canopy surface, and can be obtained using hemispherical photographs, a plant canopy analyzer, or a quantum sensor (J. M. Chen et al., 1997; Gower et al., 1999; Jonckheere et al., 2004). While there are uncertainties associated with allometric approaches, optical measures of LAI also have uncertainties related to the representativeness of observation points, light conditions, and clumping of leaves (Ryu et al., 2010). Shin et al. (2020) directly compare allometric and optical LAI at a similar Cajander larch forest in eastern Siberia, finding good agreement between the methods, and indicating that our results are comparable to those derived from optical techniques. However, this only applies to tree LAI, as obtaining optical measurements of tall shrub canopies would be challenging due to the low sensor positioning that would be required, and the difficulty associated with differentiating tree and tall shrub LAI.

Due to the apparent correlation between satellite-derived VIs and tall shrub LAI, we speculate that NDVI and EVI might be relatively accurate proxies for tall shrub LAI and biomass, but not tree LAI and biomass in these ecosystems. Though more data is necessary to determine the accuracy and consistency of this relationship, it may alter interpretations of long-term trends in VIs in locations where tree canopy cover varies. Greening and browning trends in response to warming are very well documented in the Arctic, especially at the taiga-tundra ecotone (TTE; Berner et al., 2020; Berner & Goetz, 2022; de Jong et al., 2011; Guay et al., 2014; Ju & Masek, 2016; Myers-Smith et al., 2020). Greening has been explicitly linked to the expansion of deciduous shrubs north of the

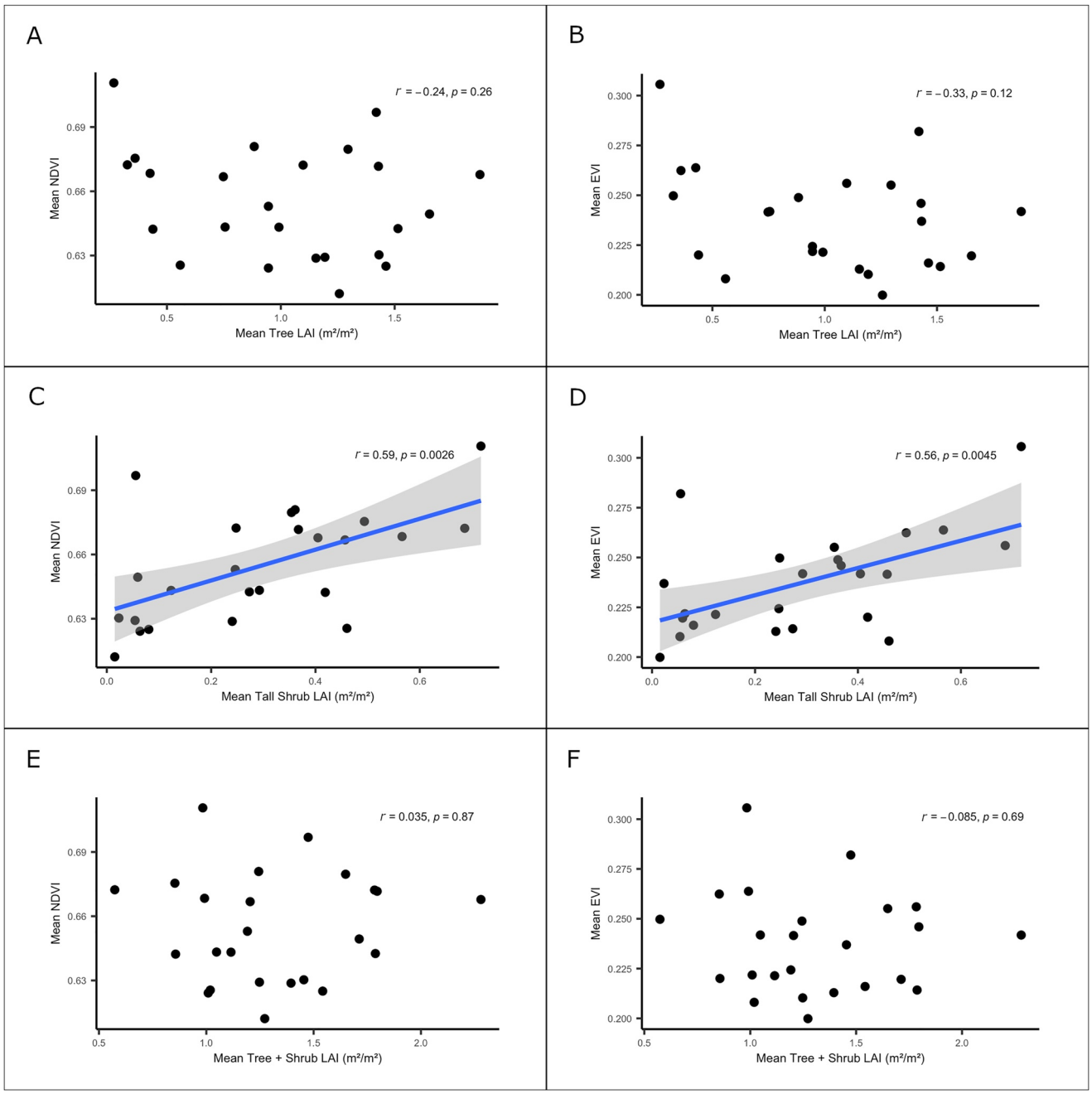

Figure 4. From Planet imagery, the relationships between mean tree LAI and NDVI (a), mean tree LAI and EVI (b), mean tall shrub LAI and NDVI (c), mean tall shrub LAI and EVI (d), mean tree + shrub LAI and NDVI (e), and mean tree + shrub LAI and EVI (f). Each plot displays the Pearson's correlation coefficient (r), and the p-value. In plots (c) and (d), where $p < 0.05$, indicating a significant relationship, a regression line is included.

TTE in Siberia, specifically to increases in *Salix* spp. growth, one of the shrubs present at our study sites (Forbes et al., 2010). Our findings concur, supporting the established link between increasing shrub growth and long-term greening trends in Siberia. The relationships between tree and tall shrub LAI and satellite-derived VIs also have potential implications for ecosystem modeling, given that the partitioning of leaf area between trees and shrubs throughout the canopy is a key assumption in many models. A better understanding of the spatial and temporal distribution of trees and tall shrubs could improve the way this vegetation is represented in ecosystem models.

As a key interface between the biosphere and the atmosphere, there are several implications of variation in leaf area for ecological modeling. Our findings illustrate how trees and tall shrubs contribute to LAI across a tree

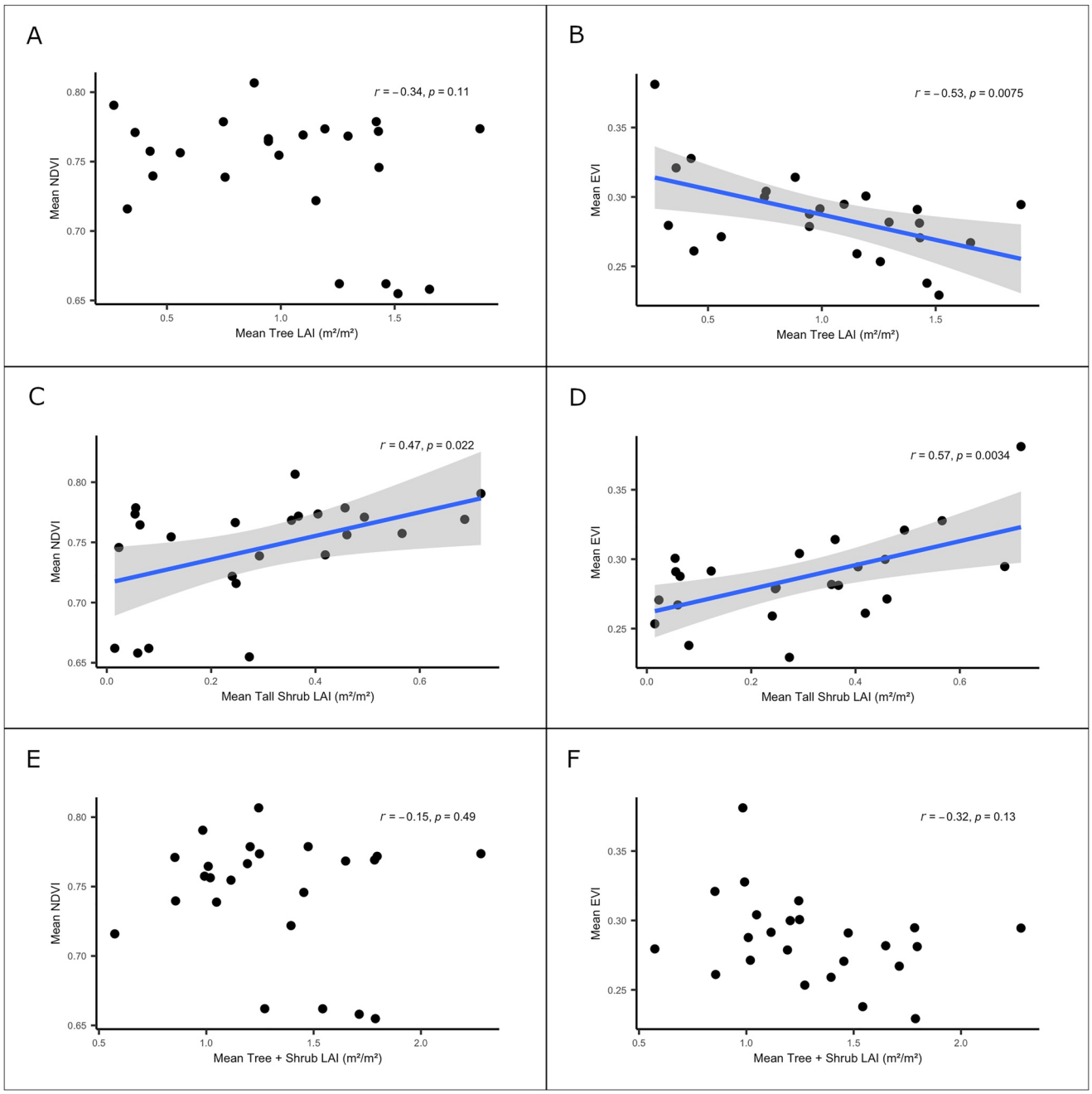

Figure 5. From Landsat imagery, the relationships between mean tree LAI and NDVI (a), mean tree LAI and EVI (b), mean tall shrub LAI and NDVI (c), mean tall shrub LAI and EVI (d), mean tree + shrub LAI and NDVI (e), and mean tree + shrub LAI and EVI (f). Each plot displays the Pearson's correlation coefficient (r), and the p-value. In plots (b), (c) and (d), where $p < 0.05$, indicating a significant relationship, a regression line is included.

density gradient in a Siberian larch forest and show that Landsat and Planet NDVI and EVI do not capture differences in forest structure due to the compensatory effects of tall shrubs in the understory. Given the substantial physiological and structural differences between trees and shrubs, accurately quantifying their relative contributions to post-fire LAI has implications for understanding a range of climatically important ecosystem processes in which woody vegetation plays a key role, including forest productivity (X. J. Walker et al., 2021), ecohydrology (Kropp et al., 2019), and soil thermal regimes (Loranty, Abbott, et al., 2018), among others. In boreal systems, VIs are typically used to infer phenology, growing season length, water and carbon dynamics, and vegetation-climate feedbacks. As VIs are typically derived from satellite imagery in this context, there is a significant amount of

uncertainty regarding what vegetation drives VIs and their spatial variation. Different assumptions regarding whether VIs are driven by trees or shrubs could lead to different interpretations and model representations of key earth system process dynamics. Our findings provide field-based measures of tree and tall shrub vegetation that demonstrates substantial abundance of tall shrub leaf area in low-density forests, as well as the subsequent need for accurate tree and tall shrub leaf area representation in models of processes such as carbon and water fluxes.

As our analyses were performed within the perimeter of a single fire, there are certainly limitations to the contexts in which they should be interpreted. Factors such as landscape history, soil conditions, and topography likely impact patterns in post-fire recruitment of trees and understory vegetation. Our results corroborate patterns of tree and shrub biomass observed across a larger geographic area encompassing many burn perimeters (Alexander et al., 2012; Webb et al., 2017), suggesting that the relationship between tree and shrub canopies likely holds true for upland Cajander larch forests in northeast Siberia. Data on tree and tall shrub variation from a wider geographic area are needed to determine the limitations of this relationship.

4.3. Potential Drivers of Variation in Tree and Shrub Leaf Area Index

Variation in burn severity across the burn perimeter is likely one of several factors driving variation in tree and tall shrub recruitment, and subsequent variation in biomass and LAI. Other potential factors include abiotic conditions (Cai et al., 2013; Johnstone, Hollingsworth, et al., 2010; Sofronov & Volokitina, 2010) and competitive interactions with other species (Dolezal, 2004; Hart & Chen, 2006; Nilsson & Wardle, 2005). During wildfire, the SOL burns unevenly, exposing the mineral soil beneath to varying degrees across the burn perimeter (Johnstone & Chapin, 2006; Johnstone & Kasischke, 2005). Alexander et al. (2018) found, using experimental burns in a nearby study area, that exposed mineral soil improves seedbed conditions for *L. cajanderi* and observed a positive relationship between burn severity and *L. cajanderi* recruitment, consistent with other research from Siberian boreal larch forests (Sofronov & Volokitina, 2010). Portions of the forest with high *L. cajanderi* recruitment rates due to higher burn severity could have lower tall shrub recruitment rates due to a more complete larch canopy, leading to smaller canopy gaps and decreased light availability for shrub establishment. However, this relationship has not been sufficiently investigated, and there could be other factors affecting shrub recruitment, depending on the mechanisms by which these shrub species recolonize a recently burned forest.

The mechanisms for post-fire recruitment of boreal shrubs are not well studied, especially in Siberia, but research from North American boreal forests has investigated these mechanisms in *Betula nana*, the most abundant shrub at our study site. *B. nana* regenerates quickly after low- and moderate-severity fire by resprouting from the surviving root crown and rhizomes, but high-severity fire kills the root crown and rhizomes, preventing resprout (de Groot et al., 1997; Racine et al., 1987). Although *B. nana* does produce wind-dispersed seeds, studies suggest that establishment from seed is rare in disturbed ecosystems (Ebersole, 1989; Whittaker, 1993). Therefore, it is possible that areas of the wildfire perimeter with higher burn severity might have high rates of *L. cajanderi* recruitment due to the high level of mineral soil exposure (Alexander et al., 2012, 2018) and low or nonexistent rates of *B. nana* sprouting due to the death of the root crown and rhizomes. Conversely, areas with lower burn severity might exhibit lower rates of *L. cajanderi* recruitment due to lower levels of mineral soil exposure (Alexander et al., 2012, 2018) and higher rates of *B. nana* sprouting due to lower levels of damage to the root crown and rhizomes. Another factor that almost certainly influences variation in tree and tall shrub recruitment is proximity to seed sources in unburned stands. Complex interactions between the many factors affecting post-fire recruitment and growth of trees and shrubs in boreal forests are likely occurring and additional research regarding the fire ecology of the trees and tall shrubs present at the site is necessary for a more conclusive explanation.

Recruitment is not the only factor that might influence variation in tree and tall shrub LAI in larch forests. Differences in tree and shrub growth rates would also affect subsequent variation in tree and shrub canopies. Studies from across northern Siberia show that *Larix* spp. growth rates have decreased with increasing temperatures over recent decades (Berner et al., 2013; Kharuk et al., 2019; Shuman et al., 2011). Research from our study sites, near the northern edge of the *L. cajanderi* range, shows that although rising temperatures are expected to generally increase tree growth, increased tree density decreases active layer depth, increasing competitive interactions and ultimately decreasing larch growth rates (X. J. Walker et al., 2021). This concurs with other findings from northeast Siberia showing overall decreases in *L. cajanderi* growth rates since the mid-twentieth century (Berner et al., 2013). In contrast, the growth rates of shrubs are increasing in response to rising temperatures in the Arctic (Myers-Smith et al., 2015). Climate change has increased the length of the growing season throughout the Arctic,

contributing to increased shrub presence across the region (Chapin et al., 2004; Euskirchen et al., 2006; Goetz et al., 2005). Evidence also suggests that specifically *Betula nana* and *Salix* spp., the two shrubs most common at our study sites, have exhibited increasing growth rates in recent decades associated with rising temperatures (Frost & Epstein, 2014; Heim et al., 2021; Stow et al., 2004; Tape et al., 2006; M. D. Walker et al., 2006). Though tall shrubs are expected to be abundant in the understory of boreal forest regardless of climatic changes, it is possible that increasing shrub growth rates due to rising temperatures influence shrub biomass and canopy cover. Further investigations into the prevalence of tall shrubs in the understory of boreal forest over time could provide insight into the potential role of climatic shifts in altering tree-shrub canopy dynamics.

5. Conclusions

We found that in a post-fire Siberian boreal larch forest, tall shrubs (>0.5 and <1.5 m) compensate for decreased tree LAI at lower density stands to create a plant canopy of consistent combined tree-shrub LAI across the density gradient. While tree LAI and tall shrub LAI individually vary significantly between high, medium, and low-density sites, variation in combined tree-shrub LAI is not significant. We also found that tall shrub LAI, but not tree LAI or combined tree-shrub LAI, was significantly and positively correlated with NDVI and EVI, indicating that tall shrub canopy cover has a greater effect on satellite-derived vegetation indices than tree or total canopy cover. Our results highlight the importance of tall shrubs in the canopy composition of regenerating boreal forests. As climate change leads to increased wildfire frequency, and as vegetation shifts toward shrub-dominated disturbance regimes across the Arctic, understanding how shrubs contribute to plant canopies will likely become increasingly critical.

Conflict of Interest

The authors declare no conflicts of interest relevant to this study.

Data Availability Statement

Data and code associated with this study are available from the Zenodo open repository (Bendavid et al., 2022).

Acknowledgments
Funding for this research was provided by the National Science Foundation (OPP-1708322, PLR-1417745, & PLR-1304464 to M.M.L., OPP-1708307 & PLR-1623764 to H.D.A., OPP-1708344 & PLR-1303940 to M.C.M., and PLR-1304007 & PLR-1417700 to S.M.N.). N.S.B. and M.M.L also received support from Colgate University. We are grateful to personnel at the Northeast Science Station for assistance in the field.

References

Abuelgasim, A. A., Fernandes, R. A., & Leblanc, S. G. (2006). Evaluation of national and global LAI products derived from optical remote sensing instruments over Canada. *IEEE Transactions on Geoscience and Remote Sensing*, *44*(7), 1872–1884. https://doi.org/10.1109/TGRS.2006.874794

Alexander, H. D., Mack, M. C., Goetz, S., Loranty, M. M., Beck, P. S. A., Earl, K., et al. (2012). Carbon accumulation patterns during post-fire succession in Cajander Larch (Larix cajanderi) forests of Siberia. *Ecosystems*, *15*(7), 1065–1082. https://doi.org/10.1007/s10021-012-9567-6

Alexander, H. D., Natali, S. M., Loranty, M. M., Ludwig, S. M., Spektor, V. V., Davydov, S., et al. (2018). Impacts of increased soil burn severity on larch forest regeneration on permafrost soils of far northeastern Siberia. *Forest Ecology and Management*, *417*, 144–153. https://doi.org/10.1016/j.foreco.2018.03.008

Bartels, S. F., & Chen, H. Y. H. (2010). Is understory plant species diversity driven by resource quantity or resource heterogeneity? *Ecology*, *91*(7), 1931–1938. https://doi.org/10.1890/09-1376.1

Bendavid, N., Loranty, M., & Samal, O. (2022). nbendavid1/siberia_lai: Tree and shrub LAI analysis from Northeast Siberia (Version v1.1.1). *Zenodo*. https://doi.org/10.5281/ZENODO.6878272

Beringer, J., Chapin, F. S., Thompson, C. C., & McGuire, A. D. (2005). Surface energy exchanges along a tundra-forest transition and feedbacks to climate. *Agricultural and Forest Meteorology*, *131*(3), 143–161. https://doi.org/10.1016/j.agrformet.2005.05.006

Berner, L. T., Alexander, H. D., Loranty, M. M., Ganzlin, P., Mack, M. C., Davydov, S. P., & Goetz, S. J. (2015). Biomass allometry for alder, dwarf birch, and willow in boreal forest and tundra ecosystems of far northeastern Siberia and north-central Alaska. *Forest Ecology and Management*, *337*, 110–118. https://doi.org/10.1016/j.foreco.2014.10.027

Berner, L. T., Beck, P. S. A., Bunn, A. G., & Goetz, S. J. (2013). Plant response to climate change along the forest-tundra ecotone in northeastern Siberia. *Global Change Biology*, a–n. https://doi.org/10.1111/gcb.12304

Berner, L. T., & Goetz, S. J. (2022). Satellite observations document trends consistent with a boreal forest biome shift. *Global Change Biology*, *28*(10), 3275–3292. https://doi.org/10.1111/gcb.16121

Berner, L. T., Massey, R., Jantz, P., Forbes, B. C., Macias-Fauria, M., Myers-Smith, I., et al. (2020). Summer warming explains widespread but not uniform greening in the Arctic tundra biome. *Nature Communications*, *11*(1), 4621. https://doi.org/10.1038/s41467-020-18479-5

Birch, L., Schwalm, C. R., Natali, S., Lombardozzi, D., Keppel-Aleks, G., Watts, J., et al. (2021). Addressing biases in arctic–boreal carbon cycling in the community land model Version 5. *Geoscientific Model Development*, *14*(6), 3361–3382. https://doi.org/10.5194/gmd-14-3361-2021

Bivand, R., Keitt, T., & Rowlingson, B. (2020). Rgdal: Bindings for the "geospatial" data abstraction library. Retrieved from https://CRAN.R-project.org/package=rgdal

Bonan, G. B., Pollard, D., & Thompson, S. L. (1992). Effects of boreal forest vegetation on global climate. *Nature*, *359*(6397), 716–718. https://doi.org/10.1038/359716a0

Bond-Lamberty, B., & Gower, S. T. (2007). Estimation of stand-level leaf area for boreal bryophytes. *Oecologia*, *151*(4), 584–592. https://doi.org/10.1007/s00442-006-0619-5

Cai, W., Yang, J., Liu, Z., Hu, Y., & Weisberg, P. J. (2013). Post-fire tree recruitment of a boreal larch forest in Northeast China. *Forest Ecology and Management*, *307*, 20–29. https://doi.org/10.1016/j.foreco.2013.06.056

Chapin, F. S., Callaghan, T. V., Bergeron, Y., Fukuda, M., Johnstone, J. F., Juday, G., & Zimov, S. A. (2004). Global change and the boreal forest: Thresholds, shifting states or gradual change? *AMBIO: A Journal of the Human Environment*, *33*(6), 361–365. https://doi.org/10.1579/0044-7447-33.6.361

Chen, J. M., & Black, T. A. (1992). Defining leaf area index for non-flat leaves. *Plant, Cell and Environment*, *15*(4), 421–429. https://doi.org/10.1111/j.1365-3040.1992.tb00992.x

Chen, J. M., & Cihlar, J. (1996). Retrieving leaf area index of boreal conifer forests using Landsat TM images. *Remote Sensing of Environment*, *55*(2), 153–162. https://doi.org/10.1016/0034-4257(95)00195-6

Chen, J. M., Rich, P. M., Gower, S. T., Norman, J. M., & Plummer, S. (1997). Leaf area index of boreal forests: Theory, techniques, and measurements. *Journal of Geophysical Research*, *102*(D24), 29429–29443. https://doi.org/10.1029/97JD01107

Chen, X., Vierling, L., Deering, D., & Conley, A. (2005). Monitoring boreal forest leaf area index across a Siberian burn chronosequence: A MODIS validation study. *International Journal of Remote Sensing*, *26*(24), 5433–5451. https://doi.org/10.1080/01431160500285142

Cohen, W. B., Maiersperger, T. K., Gower, S. T., & Turner, D. P. (2003). An improved strategy for regression of biophysical variables and Landsat ETM+ data. *Remote Sensing of Environment*, *84*(4), 561–571. https://doi.org/10.1016/S0034-4257(02)00173-6

De Groot, W. J., Thomas, P. A., & Wein, R. W. (1997). *Betula nana* L. and *Betula glandulosa* Michx. *Journal of Ecology*, *85*(2), 241–264. https://doi.org/10.2307/2960655

De Jong, R., De Bruin, S., De Wit, A., Schaepman, M. E., & Dent, D. L. (2011). Analysis of monotonic greening and browning trends from global NDVI time-series. *Remote Sensing of Environment*, *115*(2), 692–702. https://doi.org/10.1016/j.rse.2010.10.011

Dolezal, J. (2004). Tree growth and competition in a *Betula platyphylla*-Larix cajanderi post-fire forest in central Kamchatka. *Annals of Botany*, *94*(3), 333–343. https://doi.org/10.1093/aob/mch149

Ebersole, J. J. (1989). Role of the seed bank in providing colonizers on a tundra disturbance in Alaska. *Canadian Journal of Botany*, *67*(2), 466–471. https://doi.org/10.1139/b89-065

Elmendorf, S. C., Henry, G. H. R., Hollister, R. D., Björk, R. G., Boulanger-Lapointe, N., Cooper, E. J., et al. (2012). Plot-scale evidence of tundra vegetation change and links to recent summer warming. *Nature Climate Change*, *2*(6), 453–457. https://doi.org/10.1038/nclimate1465

Euskirchen, E. S., McGUIRE, A. D., Kicklighter, D. W., Zhuang, Q., Clein, J. S., Dargaville, R. J., et al. (2006). Importance of recent shifts in soil thermal dynamics on growing season length, productivity, and carbon sequestration in terrestrial high-latitude ecosystems. *Global Change Biology*, *12*(4), 731–750. https://doi.org/10.1111/j.1365-2486.2006.01113.x

Fernandes, R., Plummer, S., Nightingale, J., Frederic, B., Camacho de Coca, F., Fang, H., et al. (2014). CEOS global LAI product validation good practices. https://doi.org/10.5067/doc/ceoswgcv/lpv/lai.002

Forbes, B. C., Fauria, M. M., & Zetterberg, P. (2010). Russian Arctic warming and 'greening' are closely tracked by tundra shrub willows. *Global Change Biology*, *16*(5), 1542–1554. https://doi.org/10.1111/j.1365-2486.2009.02047.x

Frost, G. V., & Epstein, H. E. (2014). Tall shrub and tree expansion in Siberian tundra ecotones since the 1960s. *Global Change Biology*, *20*(4), 1264–1277. https://doi.org/10.1111/gcb.12406

Goetz, S. J., Bunn, A. G., Fiske, G. J., & Houghton, R. A. (2005). Satellite-observed photosynthetic trends across boreal North America associated with climate and fire disturbance. *Proceedings of the National Academy of Sciences*, *102*(38), 13521–13525. https://doi.org/10.1073/pnas.0506179102

Gower, S. T., Kucharik, C. J., & Norman, J. M. (1999). Direct and indirect estimation of leaf area index, fAPAR, and net primary production of terrestrial ecosystems. *Remote Sensing of Environment*, *70*(1), 29–51. https://doi.org/10.1016/S0034-4257(99)00056-5

Grandpré, L., Gagnon, D., & Bergeron, Y. (1993). Changes in the understory of Canadian southern boreal forest after fire. *Journal of Vegetation Science*, *4*(6), 803–810. https://doi.org/10.2307/3235618

Groisman, P. Y., Sherstyukov, B. G., Razuvaev, V. N., Knight, R. W., Enloe, J. G., Stroumentova, N. S., et al. (2007). Potential forest fire danger over Northern Eurasia: Changes during the 20th century. *Northern Eurasia Regional Climate and Environmental Change*, *56*(3), 371–386. https://doi.org/10.1016/j.gloplacha.2006.07.029

Guay, K. C., Beck, P. S. A., Berner, L. T., Goetz, S. J., Baccini, A., & Buermann, W. (2014). Vegetation productivity patterns at high northern latitudes: A multi-sensor satellite data assessment. *Global Change Biology*, *20*(10), 3147–3158. https://doi.org/10.1111/gcb.12647

Härkönen, S., Lehtonen, A., Manninen, T., Tuominen, S., & Peltoniemi, M. (2015). Estimating forest leaf area index using satellite images: Comparison of k-NN based Landsat-NFI LAI with MODIS-RSR based LAI product for Finland. Retrieved from https://jukuri.luke.fi/handle/10024/485899

Hart, S. A., & Chen, H. Y. H. (2006). Understory vegetation dynamics of North American boreal forests. *Critical Reviews in Plant Sciences*, *25*(4), 381–397. https://doi.org/10.1080/07352680600819286

Hedstrom, N. R., & Pomeroy, J. W. (1998). Measurements and modelling of snow interception in the boreal forest. *Hydrological Processes*, *12*(10–11), 1611–1625. https://doi.org/10.1002/(SICI)1099-1085(199808/09)12:10/11<1611::AID-HYP684>3.0.CO;2-4

Heim, R. J., Bucharova, A., Brodt, L., Kamp, J., Rieker, D., Soromotin, A. V., et al. (2021). Post-fire vegetation succession in the Siberian subarctic tundra over 45 years. *Science of the Total Environment*, *760*, 143425. https://doi.org/10.1016/j.scitotenv.2020.143425

Hijmans, R. J. (2020). Raster: Geographic data analysis and modeling. Retrieved from https://CRAN.R-project.org/package=raster

Hudson, S. R. (2011). Estimating the global radiative impact of the sea ice–albedo feedback in the Arctic. *Journal of Geophysical Research*, *116*(D16), D16102. https://doi.org/10.1029/2011JD015804

Johnstone, J. F., Allen, C. D., Franklin, J. F., Frelich, L. E., Harvey, B. J., Higuera, P. E., et al. (2016). Changing disturbance regimes, ecological memory, and forest resilience. *Frontiers in Ecology and the Environment*, *14*(7), 369–378. https://doi.org/10.1002/fee.1311

Johnstone, J. F., & Chapin, F. S. (2006). Effects of soil burn severity on post-fire tree recruitment in boreal forest. *Ecosystems*, *9*(1), 14–31. https://doi.org/10.1007/s10021-004-0042-x

Johnstone, J. F., Chapin, F. S., Hollingsworth, T. N., Mack, M. C., Romanovsky, V., & Turetsky, M. (2010). Fire, climate change, and forest resilience in interior Alaska. *Canadian Journal of Forest Research*, *40*(7), 1302–1312. https://doi.org/10.1139/X10-061

Johnstone, J. F., Hollingsworth, T. N., Chapin, F. S., & Mack, M. C. (2010). Changes in fire regime break the legacy lock on successional trajectories in Alaskan boreal forest. *Global Change Biology*, *16*(4), 1281–1295. https://doi.org/10.1111/j.1365-2486.2009.02051.x

Johnstone, J. F., & Kasischke, E. S. (2005). Stand-level effects of soil burn severity on postfire regeneration in a recently burned black spruce forest. *Canadian Journal of Forest Research*, *35*(9), 2151–2163. https://doi.org/10.1139/x05-087

Jonckheere, I., Fleck, S., Nackaerts, K., Muys, B., Coppin, P., Weiss, M., & Baret, F. (2004). Review of methods for in situ leaf area index determination. *Agricultural and Forest Meteorology*, *121*(1–2), 19–35. https://doi.org/10.1016/j.agrformet.2003.08.027

Ju, J., & Masek, J. G. (2016). The vegetation greenness trend in Canada and US Alaska from 1984–2012 Landsat data. *Remote Sensing of Environment*, *176*, 1–16. https://doi.org/10.1016/j.rse.2016.01.001

Kajimoto, T., Matsuura, Y., Osawa, A., Abaimov, A. P., Zyryanova, O. A., Isaev, A. P., et al. (2006). Size–mass allometry and biomass allocation of two larch species growing on the continuous permafrost region in Siberia. *Forest Ecology and Management*, *222*(1), 314–325. https://doi.org/10.1016/j.foreco.2005.10.031

Kharuk, V. I., Ranson, K. J., Petrov, I. A., Dvinskaya, M. L., Im, S. T., & Golyukov, A. S. (2019). Larch (*Larix dahurica* Turcz) growth response to climate change in the Siberian permafrost zone. *Regional Environmental Change*, *19*(1), 233–243. https://doi.org/10.1007/s10113-018-1401-z

Kropp, H., & Loranty, M. (2018). *Siberian boreal forest energy balance (ViPER (Vegetation Impacts on Permafrost) project)* (pp. 2016–2017). Cherskiy. https://doi.org/10.18739/A2M32NB2V

Kropp, H., Loranty, M. M., Natali, S. M., Kholodov, A. L., Alexander, H. D., Zimov, N. S., et al. (2019). Tree density influences ecohydrological drivers of plant–water relations in a larch boreal forest in Siberia. *Ecohydrology*, *12*(7). https://doi.org/10.1002/eco.2132

Krylov, A., McCarty, J. L., Potapov, P., Loboda, T., Tyukavina, A., Turubanova, S., & Hansen, M. C. (2014). Remote sensing estimates of stand-replacement fires in Russia, 2002–2011. *Environmental Research Letters*, *9*(10), 105007. https://doi.org/10.1088/1748-9326/9/10/105007

Launiainen, S., Guan, M., Salmivaara, A., & Kieloaho, A.-J. (2019). Modeling boreal forest evapotranspiration and water balance at stand and catchment scales: A spatial approach. *Hydrology and Earth System Sciences*, *23*(8), 3457–3480. https://doi.org/10.5194/hess-23-3457-2019

Liu, Y., Xiao, J., Ju, W., Zhu, G., Wu, X., Fan, W., et al. (2018). Satellite-derived LAI products exhibit large discrepancies and can lead to substantial uncertainty in simulated carbon and water fluxes. *Remote Sensing of Environment*, *206*, 174–188. https://doi.org/10.1016/j.rse.2017.12.024

Liu, Z., Yang, J., Chang, Y., Weisberg, P. J., & He, H. S. (2012). Spatial patterns and drivers of fire occurrence and its future trend under climate change in a boreal forest of Northeast China. *Global Change Biology*, *18*(6), 2041–2056. https://doi.org/10.1111/j.1365-2486.2012.02649.x

Loranty, M. M., Abbott, B. W., Blok, D., Douglas, T. A., Epstein, H. E., Forbes, B. C., et al. (2018). Reviews and syntheses: Changing ecosystem influences on soil thermal regimes in northern high-latitude permafrost regions. *Biogeosciences*, *15*(17), 5287–5313. https://doi.org/10.5194/bg-15-5287-2018

Loranty, M. M., Davydov, S., Kropp, H., Alexander, H., Mack, M., Natali, S., & Zimov, N. (2018). Vegetation indices do not capture forest cover variation in upland Siberian larch forests. *Remote Sensing*, *10*(11), 1686. https://doi.org/10.3390/rs10111686

Macias-Fauria, M., Forbes, B. C., Zetterberg, P., & Kumpula, T. (2012). Eurasian Arctic greening reveals teleconnections and the potential for structurally novel ecosystems. *Nature Climate Change*, *2*(8), 613–618. https://doi.org/10.1038/nclimate1558

Mack, M. C., Walker, X. J., Johnstone, J. F., Alexander, H. D., Melvin, A. M., Jean, M., & Miller, S. N. (2021). Carbon loss from boreal forest wildfires offset by increased dominance of deciduous trees. *Science*, *372*(6539), 280–283. https://doi.org/10.1126/science.abf3903

Myers-Smith, I. H., Elmendorf, S. C., Beck, P. S. A., Wilmking, M., Hallinger, M., Blok, D., et al. (2015). Climate sensitivity of shrub growth across the tundra biome. *Nature Climate Change*, *5*(9), 887–891. https://doi.org/10.1038/nclimate2697

Myers-Smith, I. H., Kerby, J. T., Phoenix, G. K., Bjerke, J. W., Epstein, H. E., Assmann, J. J., et al. (2020). Complexity revealed in the greening of the Arctic. *Nature Climate Change*, *10*(2), 106–117. https://doi.org/10.1038/s41558-019-0688-1

Myneni, R. B., Knyazikhin, Y., & Park, T. (2015). MCD15A2H MODIS/Terra+Aqua leaf area index/FPAR 8-day L4 global 500 m SIN grid V006 [Dataset]. NASA EOSDIS Land Processes DAAC. https://doi.org/10.5067/MODIS/MCD15A2H.006

Myneni, R. B., Ramakrishna, R., Nemani, R., & Running, S. W. (1997). Estimation of global leaf area index and absorbed par using radiative transfer models. *IEEE Transactions on Geoscience and Remote Sensing*, *35*(6), 1380–1393. https://doi.org/10.1109/36.649788

Nilsson, M.-C., & Wardle, D. A. (2005). Understory vegetation as a forest ecosystem driver: Evidence from the northern Swedish boreal forest. *Frontiers in Ecology and the Environment*, *3*(8), 421–428. https://doi.org/10.1890/1540-9295(2005)003[0421:UVAAFE]2.0.CO;2

Ogutu, B., Dash, J., & Dawson, T. (2012). Evaluation of leaf area index estimated from medium spatial resolution remote sensing data in a broadleaf deciduous forest in southern England, UK. *Canadian Journal of Remote Sensing*, *37*(4), 333–347. https://doi.org/10.5589/m11-043

Ollinger, S. V., Richardson, A. D., Martin, M. E., Hollinger, D. Y., Frolking, S. E., Reich, P. B., et al. (2008). Canopy nitrogen, carbon assimilation, and albedo in temperate and boreal forests: Functional relations and potential climate feedbacks. *Proceedings of the National Academy of Sciences*, *105*(49), 19336–19341. https://doi.org/10.1073/pnas.0810021105

Parajuli, A., Nadeau, D. F., Anctil, F., Parent, A.-C., Bouchard, B., Girard, M., & Jutras, S. (2020). Exploring the spatiotemporal variability of the snow water equivalent in a small boreal forest catchment through observation and modelling. *Hydrological Processes*, *34*(11), 2628–2644. https://doi.org/10.1002/hyp.13756

Paulson, A. K., Peña, H., Alexander, H. D., Davydov, S. P., Loranty, M. M., Mack, M. C., & Natali, S. M. (2021). Understory plant diversity and composition across a postfire tree density gradient in a Siberian Arctic boreal forest. *Canadian Journal of Forest Research*, *51*(5), 720–731. https://doi.org/10.1139/cjfr-2020-0483

Pearson, R. G., Phillips, S. J., Loranty, M. M., Beck, P. S. A., Damoulas, T., Knight, S. J., & Goetz, S. J. (2013). Shifts in Arctic vegetation and associated feedbacks under climate change. *Nature Climate Change*, *3*(7), 673–677. https://doi.org/10.1038/nclimate1858

Perovich, D. K., & Polashenski, C. (2012). Albedo evolution of seasonal Arctic sea ice: Aledo evolution of seasonal sea ice. *Geophysical Research Letters*, *39*(8). https://doi.org/10.1029/2012GL051432

Planet Team. (2017). Planet application program interface. In *Space for life on earth*.

Ponomarev, E. I., Kharuk, V. I., & Ranson, K. J. (2016). Wildfires dynamics in Siberian larch forests. *Forests*, *7*(6), 125. https://doi.org/10.3390/f7060125

Previdi, M., Smith, K. L., & Polvani, L. M. (2021). Arctic amplification of climate change: A review of underlying mechanisms. *Environmental Research Letters*, *16*(9), 093003. https://doi.org/10.1088/1748-9326/ac1c29

Racine, C. H., Johnson, L. A., & Viereck, L. A. (1987). Patterns of vegetation recovery after Tundra fires in Northwestern Alaska, U.S.A. *Arctic and Alpine Research*, *19*(4), 461–469. https://doi.org/10.2307/1551412

Rantanen, M., Karpechko, A. Y., Lipponen, A., Nordling, K., Hyvärinen, O., Ruosteenoja, K., et al. (2022). The Arctic has warmed nearly four times faster than the globe since 1979. *Communications Earth & Environment*, *3*(1), 1–10. https://doi.org/10.1038/s43247-022-00498-3

R Core Team. (2020). *R: A language and environment for statistical computing*. R Foundation for Statistical Computing. Retrieved from https://www.R-project.org/

Richardson, A. D., Keenan, T. F., Migliavacca, M., Ryu, Y., Sonnentag, O., & Toomey, M. (2013). Climate change, phenology, and phenological control of vegetation feedbacks to the climate system. *Agricultural and Forest Meteorology*, *169*, 156–173. https://doi.org/10.1016/j.agrformet.2012.09.012

Ryu, Y., Sonnentag, O., Nilson, T., Vargas, R., Kobayashi, H., Wenk, R., & Baldocchi, D. D. (2010). How to quantify tree leaf area index in an open savanna ecosystem: A multi-instrument and multi-model approach. *Agricultural and Forest Meteorology*, *150*(1), 63–76. https://doi.org/10.1016/j.agrformet.2009.08.007

Serbin, S. P., Ahl, D. E., & Gower, S. T. (2013). Spatial and temporal validation of the MODIS LAI and FPAR products across a boreal forest wildfire chronosequence. *Remote Sensing of Environment*, *133*, 71–84. https://doi.org/10.1016/j.rse.2013.01.022

Serreze, M. C., & Barry, R. G. (2011). Processes and impacts of arctic amplification: A research synthesis. *Global and Planetary Change*, *77*(1), 85–96. https://doi.org/10.1016/j.gloplacha.2011.03.004

Shin, N., Kotani, A., Sato, T., Sugimoto, A., Maximov, T. C., Nogovitcyn, A., et al. (2020). Direct measurement of leaf area index in a deciduous needle-leaf forest, eastern Siberia. *Polar Science*, *25*, 100550. https://doi.org/10.1016/j.polar.2020.100550

Shorohova, E., Kuuluvainen, T., Kangur, A., & Jõgiste, K. (2009). Natural stand structures, disturbance regimes and successional dynamics in the Eurasian boreal forests: A review with special reference to Russian studies. *Annals of Forest Science*, *66*(2), 201. https://doi.org/10.1051/forest/2008083

Shuman, J. K., Shugart, H. H., & O'Halloran, T. L. (2011). Sensitivity of Siberian larch forests to climate change: Siberian forest response to climate change. *Global Change Biology*, *17*(7), 2370–2384. https://doi.org/10.1111/j.1365-2486.2011.02417.x

Sofronov, M. A., & Volokitina, A. V. (2010). Wildfire ecology in continuous permafrost zone. In A. Osawa, O. A. Zyryanova, Y. Matsuura, T. Kajimoto, & R. W. Wein (Eds.), *Permafrost ecosystems* (Vol. 209, pp. 59–82). Springer Netherlands. https://doi.org/10.1007/978-1-4020-9693-8_4

Stocks, B. J., Fosberg, M. A., Lynham, T. J., Mearns, L., Wotton, B. M., Yang, Q., et al. (1998). Climate change and forest fire potential in Russian and Canadian boreal forests. *Climatic Change*, *38*(1), 1–13. https://doi.org/10.1023/A:1005306001055

Stow, D. A., Hope, A., McGuire, D., Verbyla, D., Gamon, J., Huemmrich, F., et al. (2004). Remote sensing of vegetation and land-cover change in Arctic Tundra ecosystems. *Remote Sensing of Environment*, *89*(3), 281–308. https://doi.org/10.1016/j.rse.2003.10.018

Talucci, A. C., Loranty, M. M., & Alexander, H. D. (2022). Siberian taiga and tundra fire regimes from 2001–2020. *Environmental Research Letters*, *17*(2), 025001. https://doi.org/10.1088/1748-9326/ac3f07

Tape, K., Sturm, M., & Racine, C. (2006). The evidence for shrub expansion in Northern Alaska and the Pan-Arctic: Shrub expansion in northern Alaska and pan-Arctic. *Global Change Biology*, *12*(4), 686–702. https://doi.org/10.1111/j.1365-2486.2006.01128.x

Turetsky, M. R., Bond-Lamberty, B., Euskirchen, E., Talbot, J., Frolking, S., McGuire, A. D., & Tuittila, E.-S. (2012). The resilience and functional role of moss in boreal and arctic ecosystems. *New Phytologist*, *196*(1), 49–67. https://doi.org/10.1111/j.1469-8137.2012.04254.x

Ueyama, M., Ichii, K., Iwata, H., Euskirchen, E. S., Zona, D., Rocha, A. V., et al. (2013). Upscaling terrestrial carbon dioxide fluxes in Alaska with satellite remote sensing and support vector regression: Upscaling CO_2 fluxes in Alaska. *Journal of Geophysical Research: Biogeosciences*, *118*(3), 1266–1281. https://doi.org/10.1002/jgrg.20095

Ueyama, M., Iwata, H., Harazono, Y., Euskirchen, E. S., Oechel, W. C., & Zona, D. (2013). Growing season and spatial variations of carbon fluxes of Arctic and boreal ecosystems in Alaska (USA). *Ecological Applications*, *23*(8), 1798–1816. https://doi.org/10.1890/11-0875.1

Valendik, E. N., & Ivanova, G. A. (2001). Fire regimes in the forests of siberia and far East (Pozharnye rezhimy v lesakh Sibiri i Dal'nego Vostoka). *Russian Forest Sciences (Lesovedenye)*, *4*, 69–76.

Verbyla, D. L. (2005). Assessment of the MODIS leaf area index product (MOD15) in Alaska. *International Journal of Remote Sensing*, *26*(6), 1277–1284. https://doi.org/10.1080/01431160412331330194

Vermote, E. F., Tanre, D., Deuze, J. L., Herman, M., & Morcette, J.-J. (1997). Second simulation of the satellite signal in the solar spectrum, 6S: An overview. *IEEE Transactions on Geoscience and Remote Sensing*, *35*(3), 675–686. https://doi.org/10.1109/36.581987

Walker, M. D., Wahren, C. H., Hollister, R. D., Henry, G. H. R., Ahlquist, L. E., Alatalo, J. M., et al. (2006). From the cover: Plant community responses to experimental warming across the tundra biome. *Proceedings of the National Academy of Sciences*, *103*(5), 1342–1346. https://doi.org/10.1073/pnas.0503198103

Walker, X. J., Alexander, H. D., Berner, L. T., Boyd, M. A., Loranty, M. M., Natali, S. M., & Mack, M. C. (2021). Positive response of tree productivity to warming is reversed by increased tree density at the Arctic tundra–taiga ecotone. *Canadian Journal of Forest Research*, *51*(9), 1323–1338. https://doi.org/10.1139/cjfr-2020-0466

Wang, Q., Adiku, S., Tenhunen, J., & Granier, A. (2005). On the relationship of NDVI with leaf area index in a deciduous forest site. *Remote Sensing of Environment*, *94*(2), 244–255. https://doi.org/10.1016/j.rse.2004.10.006

Webb, E. E., Heard, K., Natali, S. M., Bunn, A. G., Alexander, H. D., Berner, L. T., et al. (2017). Variability in above-and belowground carbon stocks in a Siberian larch watershed. *Biogeosciences*, *14*(18), 4279–4294. https://doi.org/10.5194/bg-14-4279-2017

Webb, E. E., Loranty, M. M., & Lichstein, J. W. (2021). Surface water, vegetation, and fire as drivers of the terrestrial Arctic-boreal albedo feedback. *Environmental Research Letters*, *16*(8), 084046. https://doi.org/10.1088/1748-9326/ac14ea

Whittaker, R. J. (1993). Plant population patterns in a glacier foreland succession: Pioneer herbs and later-colonizing shrubs. *Ecography*, *16*(2), 117–136. https://doi.org/10.1111/j.1600-0587.1993.tb00064.x

Wickham, H. (2016). *ggplot2: Elegant graphics for data analysis*. Springer-Verlag New York. Retrieved from https://ggplot2.tidyverse.org

Winton, M. (2006). Amplified Arctic climate change: What does surface albedo feedback have to do with it? *Geophysical Research Letters*, *33*(3), L03701. https://doi.org/10.1029/2005GL025244